Makara Journal of Science

Volume 26
Issue 2 *June*

Article 7

6-30-2022

Preparation of Zn/Al-chitosan Composite for the Selective Adsorption of Methylene Blue Dye in Water

Risfidian Mohadi
Faculty Mathematics and Natural Sciences, Universitas Sriwijaya, Palembang 30139, Indonesia

Patimah Mega Syah Bahar Nur Siregar
Research Center of Inorganic Materials and Complexes, Universitas Sriwijaya, Palembang 30139, Indonesia

Neza Rahayu Palapa
Research Center of Inorganic Materials and Complexes, Universitas Sriwijaya, Palembang 30139, Indonesia

Aldes Lesbani
Research Center of Inorganic Materials and Complexes, Universitas Sriwijaya, Palembang 30139, Indonesia, aldeslesbani@pps.unsri.ac.id

Recommended Citation

Mohadi, Risfidian; Siregar, Patimah Mega Syah Bahar Nur; Palapa, Neza Rahayu; and Lesbani, Aldes (2022) "Preparation of Zn/Al-chitosan Composite for the Selective Adsorption of Methylene Blue Dye in Water," *Makara Journal of Science*: Vol. 26: Iss. 2, Article 7.
DOI: 10.7454/mss.v26i2.1313
Available at: https://scholarhub.ui.ac.id/science/vol26/iss2/7

Makara Journal of Science, 26/2 (2022), 128–136
doi: 10.7454/mss.v26i2.1313

Preparation of Zn/Al-chitosan Composite for the Selective Adsorption of Methylene Blue Dye in Water

Risfidian Mohadi[1], Patimah Mega Syah Bahar Nur Siregar[1], Neza Rahayu Palapa[2], and Aldes Lesbani[2*]

1. Faculty Mathematics and Natural Sciences, Universitas Sriwijaya, Palembang 30139, Indonesia
2. Research Center of Inorganic Materials and Complexes, Universitas Sriwijaya, Palembang 30139, Indonesia

E-mail: aldeslesbani@pps.unsri.ac.id

Received January 23, 2022 | Accepted June 30, 2022

Abstract

Layered double hydroxide (LDHs) are widely used adsorbents for methylene blue removal. However, LDHs have a perishable structure that cannot be used repeatedly. Modifying LDHs with chitosan produces a strong material with a large surface area for methylene blue adsorption. Adsorption conditions were optimized by determining the adsorption isotherms and the adsorbent regeneration process. Results showed that the adsorption process was balanced in 90 min with maximum adsorption capacities of 86.207 mg/g, 35.336 mg/g, and 98.039 mg/g for Zn/Al, chitosan, and Zn/Al-chitosan, respectively. The adsorption in this study followed the Freundlich isotherm model. Regeneration analysis of the adsorbent showed that Zn/Al-chitosan can be used repeatedly in methylene blue adsorption.

Keywords: adsorption, layered double hydroxide, methylene blue, recycle of adsorbent, selectivity

Introduction

The textile industry is one of the fastest growing industries in Indonesia. However, the rapid industrial development causes environmental problems, such as dye pollution [1]. Synthetic dyes are more commonly used than natural dyes because they are cheap, easy to use, have more color variations, are stable, and resistant to the environment [2]. Dyestuffs exposed to water are difficult to degrade because synthetic compounds are complex and designed to be strong against light, chemical, and biological reactions. Thus, dye waste is difficult to remove.

Dye waste contains hazardous and toxic materials that can prevent sunlight from penetrating the aquatic environment and thus disrupt biological processes. Methylene blue (MB) is a commonly used dye in the textile industry. MB can irritate the digestive tract if ingested, cause cyanosis if inhaled, and cause skin irritation if in contact with skin [3]. Hence, the use of dyes in the environment is allowed only in low concentrations. According to the Decree of the Minister of the Environment concerning the Quality Standard for Liquid Waste (Kep-51/MENLH/10/1995), the maximum permissible concentration of MB is 5–10 mg/L. The structure of MB is shown in Figure 1.

Adsorption is a widely used method to remove dye waste in wastewater because it is simple, easy, and inexpensive [4]. Layered double hydroxides (LDHs) are commonly used adsorbents, but their adsorption capacity is small and their structure is easily damaged; thus, they cannot be used repeatedly. Mg-Fe LDH, Zn-Fe LDH, and Mn-Fe LDH have adsorption capacities of 71.942, 45.622, and 65.789 mg/g for MB, respectively [5].

The weakness of LDHs can be overcome by modifying the LDH surface with supporting materials, such as biochar [6], graphene [7], hydrochar [8], lignin [9], and chitosan Chitosan is a chitin deacetylation product that can absorb hazardous materials in wastewater. It is a long-chain polymer of glucosamine with a molecular formula of [C6H11NO4]n and a molecular weight of 2.5 × 10−5 Da. Chitosan is in the form of yellowish white flakes, odorless and tasteless [10]. Its active sites for adsorption are amino (NH2) and hydroxyl (OH) groups [11]. Chitosan can be produced from fishery waste, especially crustaceans such as shrimp, crabs, and shellfish [12].

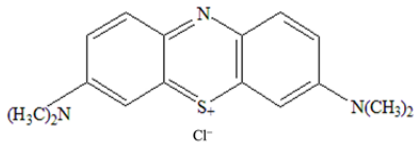

Figure 1. Chemical Structure of MB

Zn/Al-chitosan has a maximum adsorption capacity of 181.818 mg/g for Congo Red dye [13]. Meanwhile, poly(methacrylic acid) grafted-chitosan/bentonite has a maximum adsorption capacity of 110.5 mg/g for thorium(IV) removal [14]. The removal capacity of Mn-Fe LDH/CS composites for indigo carmine dye shows no significant decrease with repeated use, with removal rates of 98.80%, 91.07%, 81.29%, and 64.37% after cycles 1–4, respectively. Mn-Fe LDH/CS composites were also used to remove sunset yellow dye, with removal rates of 94.23%, 85.87%, 79.26%, and 61.98%, respectively [15].

In this study, the surface structure of layered double hydroxide (Zn/Al) was modified using chitosan extracted from shrimp shells to increase the adsorption capacity and improve the structural stability of the adsorbent so that it can be used repeatedly. The synthesized materials were characterized using XRD and FTIR analyses. The selectivity process for the dye mixture Direct Red (DR), Rhodamine-B (Rh-B), Direct Green (DG), and Methylene Blue (MB) was carried out first to determine the most selective dye. Selectivity results showed that MB was the most selective dye. Studies on the isotherms and thermodynamics of the adsorption and regeneration of the adsorbent were then performed.

Experimental Section

Chemicals and instrumentation. In this study, the materials used were $Zn(NO_3)_2.6H_2O$ (297.49 g/mol), $Al(NO_3)_3.9H_2O$ (375.13 g/mol), chitosan extracted from shrimp shells, NaOH (40 g/mol), distilled water (PT. Bratachem Indonesia), Direct Red (DR), Rhodamine-B (Rh-B), Direct Green (DG), and Methylene Blue (MB). The synthesized material was characterized using X-Ray Rigaku Miniflex-6000, FTIR by Shimadzu Prestige-21, and UV-Visible Bio-Base spectrophotometer BK-UV1800.

Synthesis of Zn/Al [16]. In this study, coprecipitation was used to synthesize Zn/Al with a molar ratio of 3:1 (0.75:0.25). $Zn(NO_3)_2{\cdot}6H_2O$ (22.3111 g, 100 mL) and $Al(NO_3)_3{\cdot}9H_2O$ (9.378 g, 100 mL) solutions were mixed in a beaker. The Zn/Al mixture was stirred 4 h at 353 K and slowly dripped with 2 M NaOH (8 g, 100 mL) until pH 10. The precipitate obtained was filtered and rinsed using distilled water. The precipitate was dried, and the solids obtained were characterized using XRD and FTIR analysis.

Extraction of Chitosan [13]. Chitosan was extracted from shrimp shells through demineralization and deproteination. Demineralization was carried out by smoothing the shrimp shells and filtered using 60 meshes. Filtered shrimp shells were placed in a 500 mL beaker and added with 1 M HCl at a ratio of 1:10 (w/v). The mixture was stirred for 3 h at 333 K, filtered, and then dried in an oven. After demineralization, deproteination was performed. The residue obtained from demineralization was placed into a beaker and added with 0.1 M NaOH at a ratio of 1:10 (w/v). The mixture was stirred for 1 h at 333 K. After the stirring was completed, the precipitate was filtered and dried in an oven at 343 K. The chitosan obtained was characterized using XRD and FTIR analysis.

Preparation of Zn/Al-chitosan [13]. $Zn(NO_3)_2{\cdot}6H_2O$ (3.33 g, 15 mL) and $Al(NO_3)_3{\cdot}9H_2O$ (1.4 g, 15 mL) solutions were mixed. The mixture was dripped with 2 M NaOH until pH 10 and stirred for 1 h. The mixture was added with chitosan (3 g) and stirred for 72 h at 353 K. The precipitate was filtered using distilled water, dried in an oven, and then characterized using XRD and FTIR analysis.

Selectivity of dyes. Dye selectivity was determined by mixing various dyes with the same concentration (20 mg/L). A mixture of dyes (DR, Rh-B, DG, and MB) was added to 0.02 g of adsorbent. The dye mixture was stirred for various times (0, 30, 60, 90, and 120 min) and measured using a UV-visible spectrophotometer at 400–700 nm wavelength range.

Concentration and temperature. The most selective dyes were used in the adsorption experiment. The effect of isotherm and adsorption thermodynamics was determined by varying the initial MB concentration and the adsorption temperature. The initial concentrations of MB were 60, 70, 80, 90, and 100 mg/L, and the adsorption temperatures were 303, 313, 323, and 333 K. The obtained filtrate was measured at the maximum wavelength of MB (664 nm) using a UV-visible spectrophotometer.

Regeneration of adsorbent. The structural stability of each adsorbent was studied through dye regeneration after desorption using an ultrasonic system. In this experiment, 0.1 g of adsorbent was used to adsorb MB (100 mg/L, 25 mL). The solution was stirred, and the filtrate was measured using a UV-visible spectrophotometer. The adsorbent containing the dye was desorbed using an ultrasonic system, and then the adsorbent was dried for 3 h at 373 K. The same treatment was carried out for the next regeneration cycle.

Results and Discussion

The synthesized material showed a typical XRD pattern and angle (Figure 2). As shown in Figure 2(a), typical peaks of LDH appeared at 10.150°(003), 19.98° (002), and 60.002°(110), indicating that the LDH structure contains layers, metal oxides from Zn-O or Al-O, and anions, respectively [13]. The results obtained were similar to the JCPDS data 48-1023. The diffraction patterns of chitosan appeared at 7.93°(003) and 19.35°(002) as shown in Figure 2(b), the XRD patterns of chitosan appeared at

9.49°(001) and 19.59°(002) [17]. The XRD pattern of Zn/Al-chitosan showed typical peaks of LDH at 9.99°(003) and 60°(110) and then a peak of chitosan at 19.97°(002) as shown in Figure 2(c). This result confirms that Zn/Al-chitosan synthesis has been successfully carried out, marked by the appearance of distinct peaks from each of the constituent materials. Zn/Al diffraction after modification with chitosan showed a shift of peaks toward smaller ones. This phenomenon can be ascribed to the addition of the interlayer distance of Zn/Al, which also increased the surface area of the material.

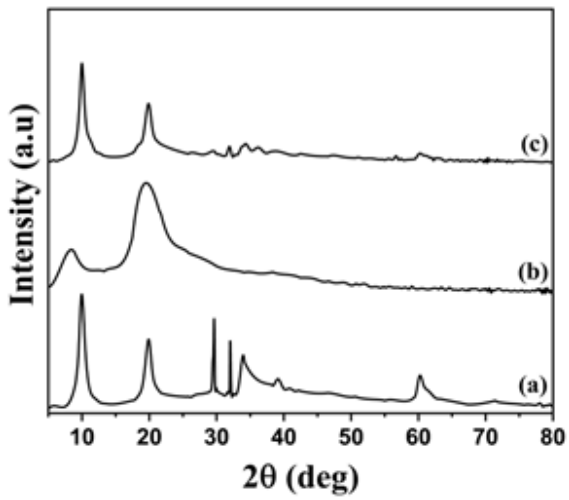

Figure 2. XRD Powder Patterns of Zn/Al (a), Chitosan (b), Zn/Al-chitosan (c)

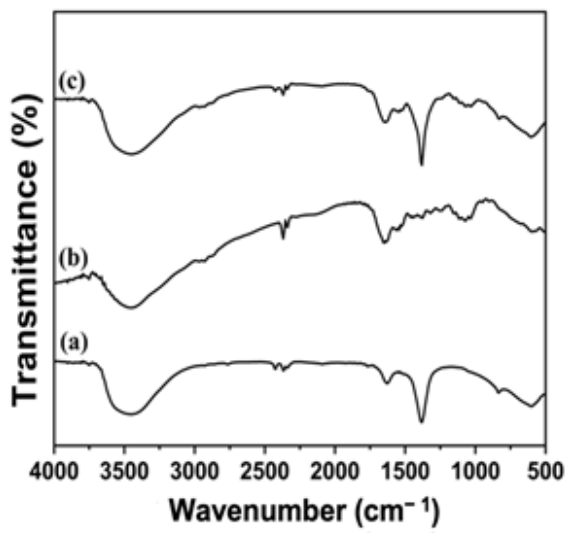

Figure 3. FTIR Spectra of Zn/Al (a), Chitosan (b), and Zn/Al-chitosan (c)

The FTIR spectra of each material are shown in Figure 3. As shown in Figure 3(a), a peak appeared at 3500 cm^{-1}, which corresponded to the stretching characteristic of water molecules and hydroxyl groups. The peaks at 1400–500 cm^{-1} corresponded to anion vibration from LDH and metal vibration with oxygen (M-O) [18]. The peak at 3447 cm^{-1} corresponded to the stretching vibrations of the NH_2 and OH groups in chitosan, as shown in Figure 3(b). Peaks at 1652 and 1566 cm^{-1} indicate the presence of $CONH_2$ and NH_2 in chitosan, respectively [19]. Zn/Al-chitosan showed typical peaks of LDH and chitosan at 3500, 1652, and 1400 cm^{-1}, as shown in Figure 3(c).

The selectivity of the dye mixture (DR, Rh-B, DG, and MB) is shown in Figure 4. As shown in the figure, the absorbance of MB was lower than those of DR, Rh-B, and DG. This result indicates that MB is the most selective dye that can be easily absorbed by the adsorbent. After 90–120 min, the decrease in MB absorption still occurred but was not significant, indicating that MB reached equilibrium.

As shown in Table 1, the adsorbed concentration of MB was greater than those of DR, Rh-B, and DG at an adsorption time of 120 min. This result suggested that MB was more easily adsorbed than DR, Rh-B, and DG.

In this study, the concentration variations were 60, 70, 80, 90, and 100 mg/L, and the adsorption temperatures were 303, 313, 323, and 333 K. Figure 5 shows that the higher the temperature used, the higher the absorption of MB. The increase in temperature increased the porosity of the adsorbent, which consequently improved its performance [20].

The interaction between the adsorbate and the adsorbent can be determined by the adsorption isotherm. The Langmuir and Freundlich isotherm equations are commonly used in adsorption. Langmuir or chemical adsorption occurs because of chemical forces and is followed by chemical reactions. In chemical adsorption, monolayer adsorption occurs. The amount of chemical adsorption energy is ±100 kJ/mol. Chemical adsorption causes the formation of chemical bonds followed by chemical reactions to produce new compounds. The chemical bonds in chemisorption allow the strong binding of gas or liquid molecules to the solid surface, rendering them difficult to be released (irreversible). Physical adsorption occurs because of physical forces and in multilayers. The amount of physical adsorption energy is ±30 kJ/mol. Physically adsorbed molecules are not strongly bound to the adsorbent surface and usually undergo a fast (reversible) reverse process, making them easily replaced with other molecules. Physical adsorption is based on Van Der Waals forces and can occur on polar and non-polar surfaces [21].

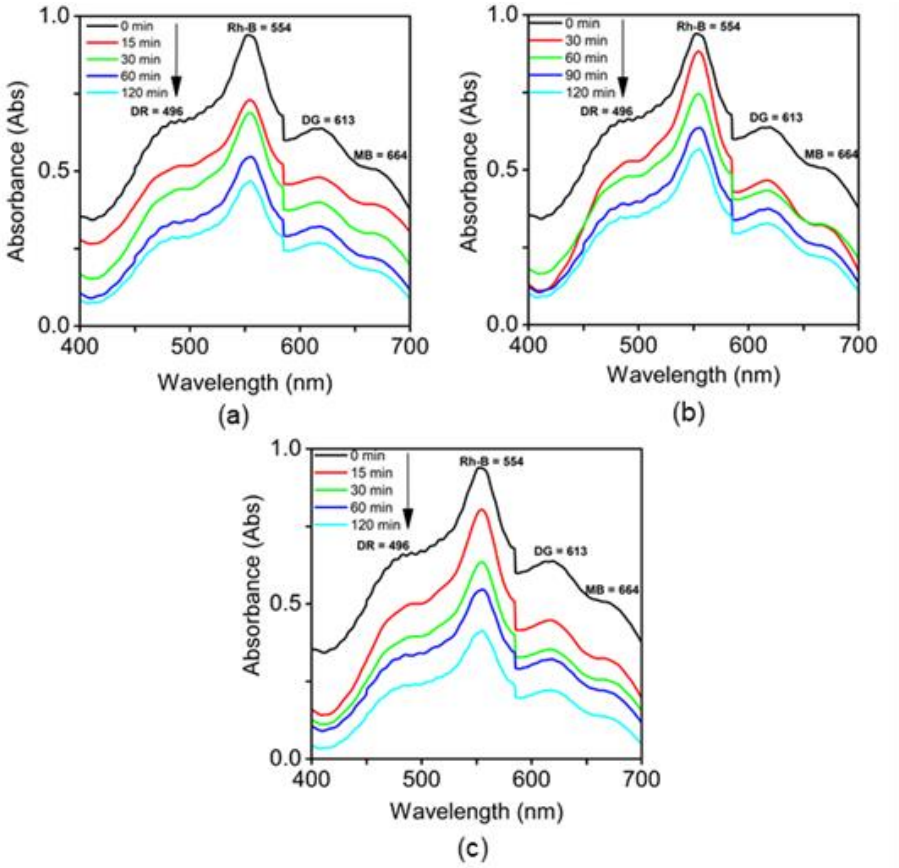

Figure 4. Selectivity of Dye Mixtures of DR, Rh-B, DG, and MB with Varying Contact Times to Zn/Al (a), Chitosan (b), and Zn/Al-chitosan (c)

Table 1. Dye Mixture Adsorbed Concentration Data on Each Adsorbent with 120 min Adsorption

Adsorbent	Adsorbed Concentration (mg/L)			
	Direct Red (DR)	Rhodamine-B (Rh-B)	Direct Green (DG)	Methylene Blue (MB)
Zn/Al	1.02	3.13	4.28	4.39
Chitosan	3.56	3.6	6.39	10.49
Zn/Al-chitosan	8.81	5.18	9.95	16.65

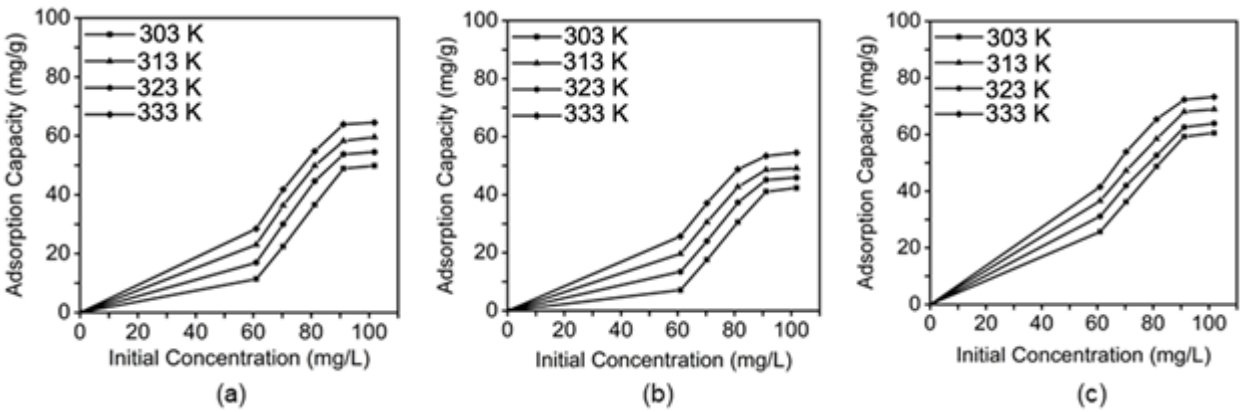

Figure 5. Effect of Initial Concentration and Adsorption Temperature of Zn/Al (a), Chitosan (b), Zn/Al-chitosan (c)

Table 2. Isotherm Adsorption

Adsorbent	Adsorption Isotherm	Adsorption Constant	T (K)			
			303	313	323	333
Zn/Al	Langmuir	Qmax	11.186	51.282	55.249	86.207
		kL	0.05	0.007	0.034	0.023
		R^2	0.8168	0.7862	0.8458	0.8737
	Freundlich	n	0.1515	0.236	0.385	1.531
		kF	1.5	1.19	6.128	1.172
		R^2	0.8947	0.8582	0.936	0.9618
Chitosan	Langmuir	Qmax	15.337	23.310	31.949	35.336
		kL	0.046	0.06	0.142	0.093
		R^2	0.9512	0.9825	0.9208	0.8219
	Freundlich	n	0.945	5.817	3.320	0.3461
		kF	1.86	8.716	1.256	2
		R^2	0.9514	0.9969	0.9916	0.9298
Zn/Al-chitosan	Langmuir	Qmax	35.336	48.077	86.957	98.039
		kL	0.093	0.008	0.078	0.037
		R^2	0.8219	0.9512	0.9591	0.8804
	Freundlich	n	0.3461	0.945	5.817	3.320
		kF	2	1.86	8.716	1.256
		R^2	0.9298	0.9514	0.9969	0.9916

Table 3. Thermodynamic Adsorption

Adsorbent	T (K)	Q_e (mg/g)	ΔH (kJ/mol)	ΔS (J/mol K)	ΔG (kJ/mol)
Zn/Al	303	48.878	19.525	0.065	-0.319
	313	53.730			-0.974
	323	58.217			-1.629
	333	63.918			-2.284
Chitosan	303	43.784	11.600	0.044	-1.805
	313	47.544			-2.248
	323	50.576			-2.690
	333	54.457			-3.133
Zn/Al-chi-tosan	303	50.455	15.920	0.052	-0.093
	313	54.457			-0.429
	323	59.551			-0.952
	333	64.524			-1.474

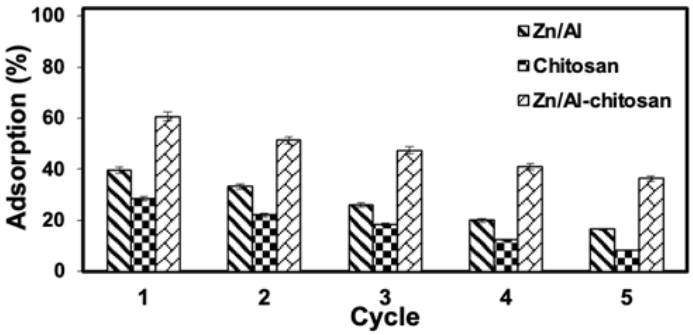

Figure 6. Regeneration of Zn/Al (a), Chitosan (b), and Zn/Al-chitosan (c)

Table 4. Methylene Blue Adsorption Capacity using Several Adsorbents

Adsorbent	Adsorption capacity (mg/g)	Reference
Ultrasonic Surface Modified Chitin	26.69	[26]
Chitosan/organic Rectorite-Fe_3O_4	24.69	[27]
Carbon Physical Activation	15.553	[28]
Activated Carbon Chemical Activation	15.478	[28]
Rice Husk	25	[29]
Kaolinite	3.4	[30]
Paper Powder	30.77	[31]
Natural Zeolite	21.189	[32]
MIP-Fe_3O_4@C_{60}@MA@IDA	41.5	[33]
Boehmite@Fe_3O_4@PLA@SiO_2	70.03	[34]
Micro Cellulose Fibrils	54.9	[35]
Mauritius Coral Limestones (MCLS)	37.24	[36]
Dried Cactus (DC)	14.045	[37]
Natural Cactus (NC)	3.435	[37]
Crystalline Hydroxyapatite Nanoparticles	14.27	[38]
SAB@Ce545	7.5	[39]
Zeolites Prepared from Egyptian Kaolins	21.4	[40]
Zn/Al	86.207	This Work
Chitosan	35.336	This Work
Zn/Al-chitosan	98.039	This Work

The adsorption pattern can be determined by a linear regression value that is closer to one in the Langmuir and Freundlich isotherms [22]. In the present study, the R^2 value for each adsorbent followed the Freundlich equation. The adsorption capacities of Zn/Al, chitosan, and Zn/Al-chitosan were 86.207, 35.336, and 98.039 mg/g, respectively, as shown in Table 2. The increase in adsorption capacity after LDH modification using chitosan can be ascribed to the fact that the active site of chitosan, namely, NH_2, can bind to the OH from LDH to form hydrogen bonds, thereby increasing the number of active sites in the adsorbent and allowing more adsorbate to be absorbed on the adsorbent surface. The results obtained suggest that Zn/Al-chitosan is an effective adsorbent for MB removal.

The adsorption thermodynamics was determined at different temperatures (303, 313, 323, and 333 K). The thermodynamic parameters determined were Gibbs free energy (ΔG), enthalpy (ΔH), and entropy (ΔS) [23, 24]. The data from the calculation of adsorption thermodynamics are listed in Table 3. A negative value of ΔG indicates that the adsorption of MB occurs spontaneously [24]. A positive value of ΔH indicates that the adsorption of MB occurs endothermically [25]. A small value of ΔS indicates a decrease in the irregularity

between the surface of the adsorbent and the adsorbate during adsorption.

Regeneration can be obtained through adsorption and desorption. Desorption releases MB from the adsorbent so that the adsorbent can be reused for the next process. This process is realized by contacting the adsorbent that has been used with distilled water through an ultrasonic system. The regeneration of each adsorbent is displayed in Figure 6. The regeneration of Zn/Al significantly decreased in cycles 4 and 5. Chitosan regeneration showed a small adsorption capacity and significantly decreased in cycles 4 and 5. Meanwhile, the regeneration of Zn/Al-chitosan was stable for up to five cycles, and its adsorption capacity was larger than those of Zn/Al and chitosan. This result confirms that Zn/Al-chitosan, given its large adsorption capacity and good repeatability, is an effective adsorbent for MB removal.

The adsorption capacities of various adsorbents for MB were compared. As shown in Table 4, the adsorption capacity of Zn/Al-chitosan was greater than those of other adsorbents.

Conclusion

The manufacture of Zn/Al-chitosan composites using LDH and chitosan extracted from shrimp shells was successfully carried out, as evidenced by XRD patterns. XRD analysis showed that Zn/Al-chitosan had a peak similar to the typical peaks of LDH at 9.99°(003) and 60°(110) and the typical peak of chitosan at 19.97°(002). The LDH modification was performed to increase the adsorption capacity and regeneration of the adsorbent. The selectivity process for the dye mixture showed that MB was more easily absorbed than other dyes. The adsorption process followed the Freundlich isothermal equation. Thermodynamic studies showed that the adsorption occurred spontaneously and endothermically, as evidenced by the negative ΔG value and ΔH value <40 kJ/mol, respectively. The small ΔS value indicated a small irregularity in the adsorption process. Regeneration showed that Zn/Al-chitosan had better capacity and stability than its constituent materials, such as layered double and chitosan.

Acknowledgments

All authors thank the Laboratory of Inorganic Materials and Complexes of the Faculty of Mathematics and Natural Sciences, Sriwijaya University for supporting this research.

References

[1] Chopra, M., Drivjot, Amita. 2012. Adsorption of Dyes from Aqueous Solution Using Orange Peels: Kinetics and Equilibrium. J. Adv. Lab. Res. Biol. 3(1): 1–8.

[2] Sadiq, A.C., Rahim, N.Y., Suah, F.B.M. 2020. Adsorption and Desorption of Malachite Green by Using Chitosan-Deep Eutectic Solvents Beads. Int. J. Biol. Macromol. 164: 3965–3973, https://doi.org/10.1016/j.ijbiomac.2020.09.029.

[3] Khodaie, M., Ghasemi, N., BabakMoradi, Rahimi, M. 2013. Removal of Methylene Blue from Wastewater by Adsorption onto ZnCl2 Activated Corn Husk Carbon Equilibrium Studies. J. Chem. 1–7, https://doi.org/10.1155/2013/383985.

[4] Liu, Y., *et al*. 2020. Rapid, Selective Adsorption of Methylene Blue from Aqueous Solution by Durable Nanofibrous Membranes. J. Chem. Eng. Data. 65(8): 3998–4008, https://doi.org/10.1021/acs.jced.0c00318.

[5] Shi, Z., Wang, Y., Sun, S., Zhang, C., Wang, H. 2020. Removal of Methylene Blue from Aqueous Solution Using Mg-Fe, Zn-Fe, Mn-Fe Layered Double Hydroxide. Water Sci. Technol. 81(12): 2522–2532, https://doi.org/10.2166/wst.2020.313.

[6] Lyu, P., Wang, G., Wang, B., Yin, Q., Li, Y., Deng, N. 2021. Adsorption and Interaction Mechanism of Uranium (VI) from Aqueous Solutions on Phosphate-Impregnation Biochar Cross-Linked Mg–Al Layered Double-Hydroxide Composite. Appl. Clay Sci. 209: 106146, https://doi.org/10.1016/j.clay.2021.106146.

[7] Yu, Y., Sun, R., Wang, Z., Yao, M., Wang, G. 2021. Self-Supported Graphene Oxide/Sodium Alginate/1, 2-Propanediamine Composite Membrane and Its Pb2+ Adsorption Capability. J. Environ. Chem. Eng. 9(5): 106254, https://doi.org/10.1016/j.jece.2021.106254.

[8] Luo, X., *et al*. 2020. Hydrothermal Carbonization of Sewage Sludge and in-Situ Preparation of Hydrochar/MgAl-Layered Double Hydroxides Composites for Adsorption of Pb(II). J. Cleaner Prod. 258: 120991, https://doi.org/10.1016/j.jclepro.2020.120991.

[9] Castillo, R.O., Doumer, M.E., Arízaga, G.G.C., Hernández, A.D., Hermosillo, C.G. 2018. Spectroscopic Study of Copper Adsorption by Chitosan and Lignin Composites Containing Layered Double Hydroxides. J. Electron Spectrosc. Relat. Phenom. 226: 1–8, https://doi.org/10.1016/ j.elspec.2018.04.004.

[10] Ge, H., Du, J. 2020. Selective Adsorption of Pb(II) and Hg(II) on Melamine-Grafted Chitosan. Int. J. Biol. Macromol. 162: 1880–1887, https://doi.org/10.1016/j.ijbiomac.2020.08.070.

[11] Kloster, G.A., Valiente, M., Marcovich, N.E., Mosiewicki, M.A. 2020. Adsorption of Arsenic Onto Films Based on Chitosan and Chitosan/Nano-Iron Oxide. Int. J. Biol. Macromol. 165: 1286–1295, https://doi.org/10.1016/j.ijbiomac.2020.09.244.

[12] Seedao, C., Rachphirom, T., Phiromchoei, M., Jangiam, W. 2018. Anionic Dye Adsorption from Aqueous Solutions by Chitosan Coated Luffa Fibers.

ASEAN J. Chem. Eng. 18(2): 31–40, https://doi.org/10.22146/ajche.49534.

[13] Siregar, P.M.S.B.N., Normah, Juleanti, N., Wijaya, A., Palapa, N.R., Mohadi, R., Lesbani, A. 2021. Mg/Al-CH, Ni/Al-CH and Zn/Al-CH as Adsorbents for Congo Red Removal in Aqueous Solution. Commun. Sci. Technol. 6(2): 74–79, https://doi.org/10.21924/cst.6.2.2021.547.

[14] Anirudhan, T.S., Rijith, S., Tharun, A.R. 2010. Adsorptive Removal of Thorium(IV) from Aqueous Solutions Using Poly(Methacrylic Acid)-Grafted Chitosan/Bentonite Composite Matrix: Process Design and Equilibrium Studies. Colloid Surf. A-Physicochem. Eng. Asp. 368(3): 13–22, https://doi.org/10.1016/j.colsurfa.2010.07.005.

[15] Khalili, R., Ghaedi, M., Parvinnia, M., Sabzehmeidani, M.M. 2021. Simultaneous Removal of Binary Mixture Dyes Using Mn-Fe Layered Double Hydroxide Coated Chitosan Fibers Prepared by Wet Spinning. Surf. Interfaces. 23: 100976, https://doi.org/10.1016/j.surfin.2021.100976.

[16] Karami, Z., *et al*. 2019. Epoxy/Layered Double Hydroxide (LDH) Nanocomposites: Synthesis, Characterization, and Excellent Cure Feature of Nitrate Anion Intercalated Zn-Al LDH. Prog. Org. Coat. 136: 1–6, https://doi.org/10.1016/j.porgcoat.2019.105218.

[17] Sugiyanti, D., Anggrahini, S., Pranoto, Y., Anwar, C., Santoso, U. 2019. Low Molecular Weight Chitosan from Shrimp Shell Waste using Steam-Explosion Process Under Catalyst of Phosphotungstic Acid. Orient. J. Chem. 35(1): 193–199, http://dx.doi.org/10.13005/ojc/350122.

[18] Benício, L.P.F., *et al*. 2015. Layered Double Hydroxides: Nanomaterials for Applications in Agriculture | Hidróxidos Duplos Lamelares: Nanomateriais Para Aplicações Na Agricultura. Rev. Bras. Cienc. Solo. 39(1): 1–13, https://doi.org/10.1590/01000683rbcs2015081.

[19] Lustriane, C., Dwivany, F.M., Suendo, V., Reza, M. 2018. Effect of Chitosan and Chitosan-Nanoparticles on Post Harvest Quality of Banana Fruits. J. Plant Biotechnol. 45: 36–44, https://doi.org/10.5010/JPB.2018.45.1.036.

[20] Suhendrayatna, Zaki, M., Harahap, A.D.H., Verantika, F. 2018. Adsorption of Manganese(II) Ion in the Water Phase by Citric Acid Activated Carbon of Rice Husk. Emerald Reach Proceedings Series. 1(2): 547–554, https://doi.org/10.1108/978-1-78756-793-1-00089.

[21] Siregar, P.M.S.B.N., Palapa, N.R., Wijaya, A., Fitri, E.S., Lesbani, A. 2021. Structural Stability of Ni/Al Layered Double Hydroxide Supported on Graphite and Biochar Toward Adsorption of Congo Red. Sci. Technol. Indonesia. 6(2): 85–95, https://doi.org/10.26554/sti.2021.6.2.85-95.

[22] Wijaya, A., Siregar, P.M.S.B.N., Priambodo, A., Palapa, N.R., Taher, T., Lesbani, A. 2021. Innovative Modified of Cu-Al/C (C = Biochar, Graphite) Composites for Removal of Procion Red from Aqueous Solution. Sci. Technol. Indonesia. 6(4): 228–234, https://doi.org/10.26554/sti.2021.6.4.228-234.

[23] Mohadi, R., Normah, Fitri, E.S., Palapa, N.R. 2022. Unique Adsorption Properties of Cationic Dyes Malachite Green and Rhodamine-B on Longan (*Dimocarpus longan*) Peel. Sci. Technol. Indonesia. 7(1): 115–125, https://doi.org/10.26554/sti.2022.7.1.115-125.

[24] Wong, S., *et al*. 2020. Effective Removal of Anionic Textile Dyes Using Adsorbent Synthesized from Coffee Waste. Sci. Rep. 10(1): 1–13, https://doi.org/10.1038/s41598-020-60021-6.

[25] Ashraf, M.W., Abulibdeh, N., Salam, A. 2019. Adsorption Studies of Textile Dye (Chrysoidine) from Aqueous Solutions Using Activated Sawdust. Int. J. Chem. Eng. 1–9, https://doi.org/10.1155/2019/9728156.

[26] Dotto, G.L., Santos, J.M.N., Rodrigues, I.L., Rosa, R., Pavan, F.A., Lima, E.C. 2015. Adsorption of Methylene Blue by Ultrasonic Surface Modified Chitin. J. Colloid Interface Sci. 446: 133–140, https://doi.org/10.1016/j.jcis.2015.01.046.

[27] Zeng, L., *et al*. 2015. Chitosan/organic Rectorite Composite for The Magnetic Uptake of Methylene Blue and Methyl Orange. Carbohydr. Polym. 123: 89–98, https://doi.org/10.1016/j.carbpol.2015.01.021.

[28] Khuluk, R.H., Rahmat, A., Buhani, Suharso. 2019. Removal of Methylene Blue by Adsorption onto Activated Carbon From Coconut Shell (*Cocous Nucifera* L.). Indonesian J. Sci. Technol. 4(2): 229–240, https://doi.org/10.17509/ijost.v4i2.18179.

[29] Patil, M.A., Shinde, J.K., Jadhav, A.L., Deshpande, S.R. 2017. Adsorption of Methylene Blue in Waste Water by Low Cost Adsorbent Rice Husk. Adsorpt. 10(1): 246–252.

[30] Sagita, C.P., Nulandaya, L., Kurniawan, Y.S. 2021. Efficient and Low-Cost Removal of Methylene Blue using Activated Natural Kaolinite Material. J. Multidiscip. Appl. Nat. Sci. 1(2): 69–77, https://doi.org/10.47352/jmans.v1i2.80.

[31] Labiebah, G., Djunaidi, M.C., Haris, A., Widodo, D. 2019. Removal of Methylene Blue Using Used Paper Powder. Jurnal Kimia, Sains dan Aplikasi. 22(1): 23–28, https://doi.org/10.14710/jksa.22.1.23-28.

[32] Gago, J., Ngapa, Y.D. 2021. Optimizing of Competitive Adsorption Methylene Blue and Methyl Orange using Natural Zeolite from Ende-Flores. Jurnal Kimia dan Pendidikan Kimia. 6(1): 39–48, https://doi.org/10.20961/jkpk.v6i1.46132.

[33] Xu, H., Zhang, P., Zhou, S.Y., Jia, Q. 2020. Fullerene Functionalized Magnetic Molecularly Imprinted Polymer: Synthesis, Characterization and Application for Efficient Adsorption of Methylene Blue. Chin. J. Anal. Chem. 48(9): e20107–e20113, https://doi.org/10.1016/S1872-2040(20)60045-7.

[34] Alinezhad, H., Zabihi, M., Kahfroushan. D. 2020. Design and Fabrication The Novel Polymeric Magnetic Boehmite Nanocomposite (Boehmite@ Fe3O4@PLA@SiO2) for The Remarkable Competitive Adsorption of Methylene Blue and Mercury Ions. J. Phys. Chem. Solids. 144: 109515, https://doi.org/10.1016/j.jpcs.2020.109515.

[35] Kankılıç G.B., Metin, A.Ü. 2020. Phragmites Australis as a New Cellulose Source: Extraction, Characterization and Adsorption of Methylene Blue. J. Mol. Liq. 312: 1–10, https://doi.org/ 10.1016/j.molliq.2020.113313.

[36] Nkutha, C.S., Shooto, N.D., Naidoo, E.B. 2020. Adsorption Studies of Methylene Blue and Lead Ions from Aqueous Solution by Using Mesoporous Coral Limestones. S. Afr. J. Chem. Eng. 34: 151–157, https://doi.org/10.1016/j.sajce.2020.08.003.

[37] Sakr, F., Alahiane, S., Sennaoui, A., Dinne, M., Bakas, I., Assabbane, A. 2019. Removal of Cationic Dye (Methylene Blue) from Aqueous Solution by Adsorption on Two Type of Biomaterial of South Morocco. Mater. Today Proc. 22: 93–96, https://doi.org/10.1016/j.matpr.2019.08.101.

[38] Wei, W., Yang, L., Zhong, W.H., Li, S.Y., Cui, J., Wei, Z.G. 2015. Fast Removal of Methylene Blue from Aqueous Solution by Adsorption Onto Poorly Crystalline Hydroxyapatite Nanoparticles. Dig. J. Nanomater. Biostruct. 10(4): 1343–1363.

[39] Jabli, M., Almalki, S.G., Agougui, H. 2019. An Insight Into Methylene Blue Adsorption Characteristics Onto Functionalized Alginate Bio-Polymer Gel Beads with λ-Carrageenan-Calcium Phosphate, Carboxymethyl Cellulose, and Celite 545. Int. J. Biol. Macromol. 156: 1091–1103, https://doi.org/10.1016/j.ijbiomac.2019.11.140.

[40] EL-Mekkawi, D.M., Ibrahim, F.A., Selim, M.M. 2016. Removal of Methylene Blue from Water Using Zeolites Prepared from Egyptian Kaolins Collected from Different Sources. J. Environ. Chem. Eng. 4(2): 1417–1422, https://doi.org/10.1016/j.jece.2016.01.007.